富山大学水素同位体科学研究センター研究報告 26 : 1 −12, 2006.

論文

Kinetics of Methane Decomposition over Zr-Ni Alloys

K. Watanabe, W. Shu* and M. Matsuyama
Hydrogen Isotope Research Center, University of Toyama
Gofuku 3190, Toyama 930-8555, Japan
* Present Affiliation: Tritium Process Laboratory, JAERI, Japan

Received May 18th, 2007; accepted June 29th, 2007

ABSTRACT

The decomposition of methane over Zr, Zr_4Ni and Zr_2Ni was investigated to develop highly active materials for capturing tritiated methane inevitably formed in tritium handling systems. The entire decomposition or absorption curves, however, could not been described by any simple kinetic equations appearing in the literature. The present paper describes verification of plausible kinetic equations reproducing the observed absorption curves, assuming a reaction mechanism consisting of a progressive removal of hydrogen atoms according to $CH_4(g) \rightarrow CH_3(a) \rightarrow CH_2(a) \rightarrow CH(a) \rightarrow C(a)$ and its modification including carbon segregation schemes by solving a set of kinetic equations by means of finite difference method, by taking into account of ab-initio calculations of potential energy surfaces by Gaussian 03.

It was found that a step-by-step H-deletion model could not generate the experimentally observed absorption curves, but they could be reproduced quite well in the whole reaction range by a modified reaction scheme assuming coagulation of a carbon residue like $CH_2(a)$ or $CH(a)$ to carbonaceous deposits, described as $CH_4(g) \xrightarrow{k_1} CH_3(a) \xrightarrow{k_2} CH(a) \xrightarrow{k_3}$ C-deposits. It was concluded that the final third step (with a rate constant of k_3) governs the overall absorption reactivity (methane consumption beyond 90%) of the materials.

1. Introduction

In tritium handling facilities including those processing tritium for thermonuclear reactors, tritium gas is contaminated by many impurity gases generated during tritium handling. Typical gaseous impurities found in various tritium systems are CQ_4, CO, CO_2, O_2, N_2, NQ_3 and Q_2O, where Q denotes H, D or T atom. They should be removed from the gaseous stream and tritium recovered from the impurity gases should be made available for reuse or stored in stable form. Metallic compounds consisting of Zr and some transition elements have been proved to be quite promising for storage, supply and recovery of tritium in tritium handling systems[1]. They can easily absorb tritium not only in the elemental form but also in form of water, ammonia and gaseous hydrocarbons as well as non-radioactive impurity species such as CO, CO_2, O_2 and N_2. Among them it is most difficult to recover tritium from hydrocarbons, especially methane. In general, tritium included in hydrocarbons could be recovered by catalytic isotope exchange reactions, but the procedures are rather complicated. Some of metallic compounds consisting of Zr and transition metals (hereafter denominated as Zr-alloys) can be used to decompose hydrocarbons and capture tritium at the same time. To decompose hydrocarbons and to capture tritium bound to carbon, however, it is required to heat up the metallic compounds

to rather high temperature. Among the hydrocarbons, methane is most inactive with these metallic compounds and requires higher temperature than the others[2, 3].

The present authors have investigated the usefulness of Zr-alloys for handling tritium gas containing gaseous impurities[1] and found that Zr-Ni alloys are most promising for removing tritium from tritiated methane[1, 4, 5]. According to the studies, Zr_4Ni is most active for decomposing methane among other alloys as Zr_2Ni, ZrNi and Zr_7Ni_{11} and pure Zr. In these studies, however, the activity was evaluated from the linear part of ln P vs time plots of the absorption curves. But the absorption curves themselves were quite complicated and did not obey the first order kinetics nor other analytically known kinetic equations. It is considerably important, however, to analyze the absorption curves as low as 0.1% of the initially loaded amount of methane or below to predict the behavior of methane decomposition and the removal to a trace level, because the permissible level of tritated methane in the environment is very much lower than that of other chemical forms of tritium.

The present paper describes a model for analyzing the absorption curves of methane by Zr-Ni alloys to obtain relevant kinetic parameters. Simulated absorption curves by use of these kinetic parameters were compared with the observed ones.

2. Experimentals

Although the experimental apparatus, procedures and results obtained with some Zr-Ni alloys have been described in previous papers[1, 4, 5], a brief description of experimental procedures is given below for readers convenience.

The sample materials used were Zr_4Ni, Zr_2Ni, ZrNi and Zr_7Ni_{11} and pure Zr. X-ray diffraction measurements showed that while Zr_2Ni, ZrNi and Zr_7Ni_{11} were single-phase metallic compounds, Zr_4Ni consisted of a mixture of Zr_2Ni and Zr. They were used as powder of 200 mesh (below 74 μm). According to BET measurements using Kr, the specific surface area was 0.30, 0.24 and 0.10 m^2/g for Zr_7Ni_{11}, ZrNi and Zr_2Ni, respectively. Decomposition/absorption curves of methane over these materials were measured by constant volume method, and the absorption curves were given by the pressure as a function of time, $P(t) - t$, where 0.5 grams of powder were used for all the samples. Prior to the absorption measurements, the sample powder was heated at 423 K for 2 hours under vacuum and then at 873 K for 2 hours as the standard activation procedures in the apparatus whose residual pressure was routinely below 2.67×10^{-6} Pa.

Methane absorption/decomposition curves were measured by constant volume method, where the initial pressure was set at 13.3 Pa in the reaction cell of 173 cc.

3. Results and Discussion

3.1. Methane Absorption Curves

Figure 1 shows the absorption curves of methane for Zr, as example, at temperatures from 350 to 550 C, where the abscissa shows the reaction time in second and the ordinate the number of methane molecules in mmol in the reaction vessel of 173 cc. As seen in the figures, the number of methane molecules in the reaction chamber decreased with reaction time. It is evident, however, that the absorption curves do not obey simple first order kinetics. It is also seen that the charged methane amounting to 1 mmol almost disappeared from the gas phase at high temperatures in these runs. Thus, the total amount of methane reduction exceeded the total number of surface site on the Zr sample. For this condition it was assumed that the density of active sites is of the order of 10^{14} sites/cm^2. This indicates that methane is decomposed to hydrogen and carbon or carbon residues. As will be shown below, whereas hydrogen is absorbed in the bulk of the sample, carbon remains on the surface. This is also true for the other sample alloys.

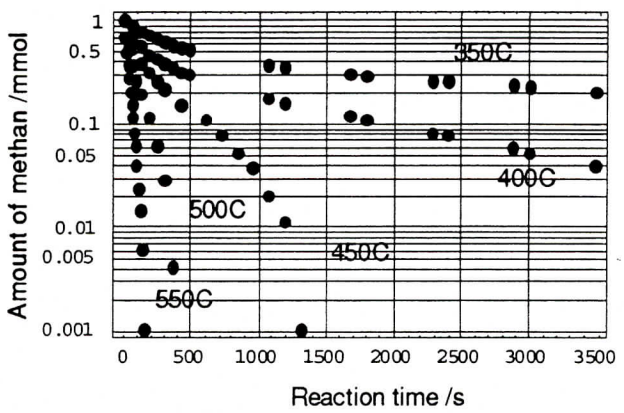

Fig. 1. Absorption curves of methane for Zr at 350, 400, 450, 500 and 550 C

The fact that the absorption curves do not obey simple first order kinetics suggests that the decomposition of methane takes place in a series of consecutive reactions. Accordingly the absorption curves should be described by a succession of elementary reactions.

3.2. Elementary Reactions on the Surface

The elementary reactions are considered to consist of a dissociative adsorption of methane and a subsequent dehydrogenation of the adsorbates. For example, a methane molecule is expected to be adosrbed on Zr-surface through the following elementary reactions as:

$$CH_4 + 4\,Zr \rightarrow Zr\text{-}CH + 3\,Zr\text{-}H \quad (1)$$

$$CH_4 + 3\,Zr \rightarrow Zr\text{-}CH_2 + 2\,Zr\text{-}H \quad (2)$$

$$CH_4 + 2\,Zr \rightarrow Zr\text{-}CH_3 + Zr\text{-}H \quad (3)$$

With respect to the subsequent steps, the elementary reactions described below should be taken into account;

$$Zr\text{-}CH + Zr \rightarrow Zr\text{-}C + Zr\text{-}H \quad (4)$$

$$Zr\text{-}CH_2 + 2\,Zr \rightarrow Zr\text{-}C + 2\,Zr\text{-}H, \quad (5)$$

$$\text{or} \quad Zr\text{-}CH_2 + Zr \rightarrow Zr\text{-}CH + Zr\text{-}H \quad (6)$$

$$Zr\text{-}CH_3 + 2\,Zr \rightarrow Zr\text{-}CH + 2\,Zr\text{-}H, \quad (7)$$

$$\text{or} \quad Zr\text{-}CH_3 + Zr \rightarrow Zr\text{-}CH_2 + Zr\text{-}H \quad (8)$$

Namely, the kinetic parameters of the reactions from (1) to (8) are required to analyze the methane absorption curves. To the author's knowledge, however, no such kinetic parameters have been reported so far. Accordingly the preference of competitive elementary reactions such as (1) ,(2) and (3), for example, was examined by ab-inito calculation of potential energy surface by using Gaussian 03[6], and it was assumed that the most likely reaction is the elementary reaction having the smallest activation energy. The calculation was carried out by using small clusters of Zr hcp crystal, where the details of the calculation have been described elsewhere[7, 8].

3.3. Potential Energy Surfaces for methane adsortion

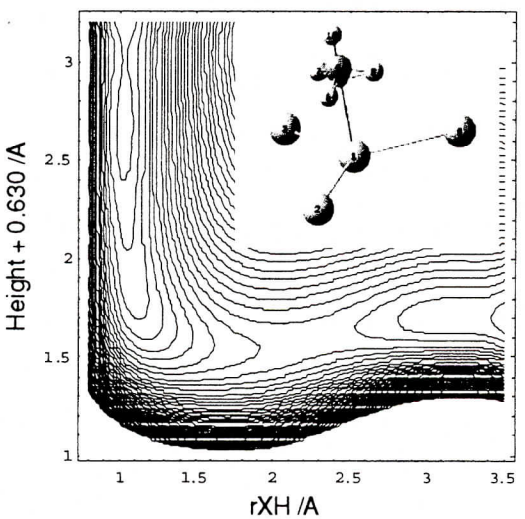

Fig. 2. Cluster model and contour map of PES for Zr4-CH_4

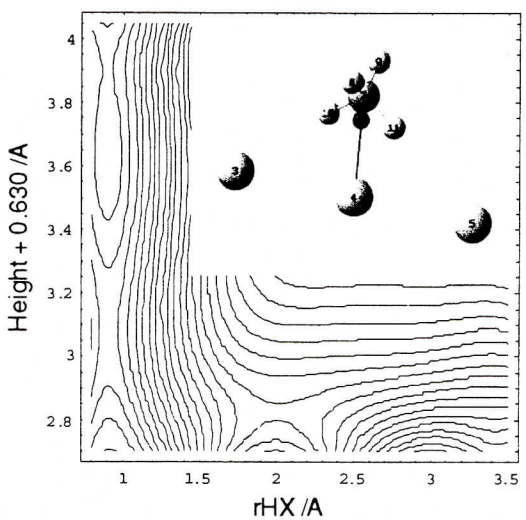

Fig. 3. Cluster model and contour map of PES for Zr3-CH_4

The potential energy surface (PES) for the adsorption of methane was calculated by adopting small clusters for modeling the Zr (1000) surface, where a set of four Zr atoms was selected for reaction (1), three Zr-atoms for reaction (2) and two atoms for reaction (3).

Figrues 2, 3 and **4** show the cluster models and contour maps of PES for Zr4-CH_4, Zr3-CH_4 and Zr2-CH_4, respectively. The first one corresponds to elementary reaction (1), the second to reaction (2) and the third to reaction (3). The model cluster for reaction (1) consists of four Zr atoms, where one Zr atom

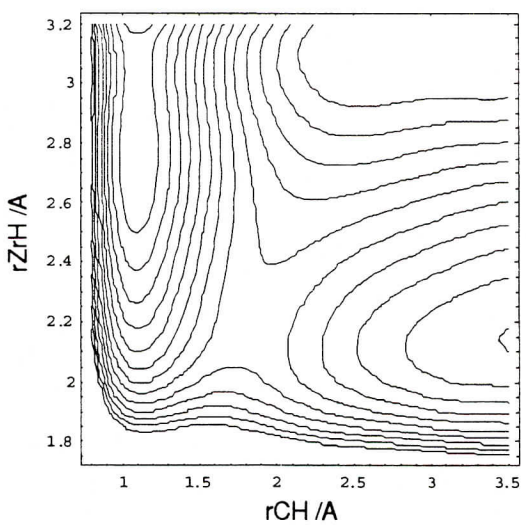

Fig. 4. Cluster model and contour map of PES for Zr2-CH_4

corresponds to the center atom of the (0001) plane of hcp-Zr, and the other three atoms are selected from every other site of the hexagonal. For reaction (2), the Zr-cluster was made by selecting three Zr atoms from a basal axis of the plane, for example [11$\bar{2}$0]. With respect to the last one, a set of two Zr atoms of nearest neighbor on (0001) plane forms the adsorption site. PES surfaces for reactions (1) and (2) were calculated by changing the distance between the dummy atom (shown by the purple sphere) and Zr1 atom (to be denoted as *height* hereafter), and that between the dummy and a hydrogen atom (H3 for reaction (1) and H10 for reaction (2)). As for reaction (3), PES was calculated by changing the distances of C-Zr and C-H. In the PES diagrams of Figs.2 and 3, the abscissa represents the separation between the dummy and the hydrogen atoms (denoted as rXH below), and the ordinate gives the distance between C and Zr atoms, where the unit of both the abscissa and the ordinate is given in $\mathring{A}$. In these cases, the distance between C and Zr1 atoms is given by the *height* + 0.630 $\mathring{A}$. Concerning the PES in Fig.4, the abscissa shows the bond distance of C-H, and the ordinate that of C-Zr.

It is seen in the contour maps that no apparent potential well appears for methane to approach the surface for reactions (1) and (2), or the potential well is very shallow as seen in Fig. 2. These results suggest that no stable adsorbed state of CH_4 is formed. Methane molecules approaching the surface are reflected or surmount the potential barrier to be dissociatively adsorbed. The potential barriers for the dissociative adsorption of CH_4 were evaluated to be 2.35, 3.72 and 2.59 eV for reactions (1), (2) and (3), respectively. Similar calculations were carried out for reactions (4) - (8) and gave the activation energies of 1.45 eV for reaction (4), 3.15 eV for reaction (5), 1.14 eV for reaction (6), 1.41 eV for reaction (7) and 2.07 eV for reaction (8).

3.4. Analysis of Absorption Curves

3.4.1. Examination of kinetic equations

According to the results described above, a reaction scheme consisting of reactions (1) and (4) was considered to be probable. Accordingly the methane absorption by Zr would proceed via the following processes

$$\underset{n(CH_4)}{CH_4(g)} + 4\,S \xrightarrow{k_1} \underset{n_{CH}}{S\text{-}CH(a)} + 3\,\underset{n_H}{S\text{-}H(a)} \tag{9}$$

$$S\text{-}CH(a) + S \xrightarrow{k_2} \underset{n_C}{S\text{-}C(a)} + S\text{-}H(a) \tag{10}$$

$$S\text{-}C(a) \xrightarrow{diffusion\ into\ bulk} C(soln) \tag{11}$$

$$S\text{-}H(a) \xrightarrow{diffusion\ into\ bulk} H(soln) \tag{12}$$

where S denotes an active site for adsorption, and (g) and (a) represent gaseous and adsorbed states, respectively. The final products of methane decomposition, i.e. C(a) and H(a), are supposed to diffuse into the bulk.

The diffusion constant of carbon into Zr in the temperature range adopted in the present

study is, however, rather small [9]. Therefore the diffusion of carbon into bulk should play no important role. In addition, the diffusion of hydrogen is also considered to play a negligible role on the absorption kinetics, because it is extremely fast under the present experimental conditions[10]. Consequently, the following equations were expected to describe the methane absorption curves by Zr:

$$-(\frac{n_{\mathrm{CH_4}}}{d\,t}) = k_1 n_{\mathrm{CH_4}}(s_0 - n_{CH} - n_C)^4 \tag{13}$$

$$(\frac{n_{CH}}{d\,t}) = k_1 n_{CH_4}(s_0 - n_{CH} - n_C)^4 - k_2 n_{CH}(s_0 - n_{CH} - n_C) \tag{14}$$

$$(\frac{n_C}{d\,t}) = k_2 n_{CH}(s_0 - n_{CH} - n_C) \tag{15}$$

where s_0 represents the number of active sites on the surface and n_X denotes the number of molecules of species X (X = CH_4, CH, or C). Absorption curves were analyzed by solving the above simultaneous differential equations by finite difference scheme through trial-and-error curve fitting, where k_1 could be determined from the slope of the very initial part of respective absorption curves and k_2 was treated as a fitting parameter. It was found, however, that the above scheme could not reproduce any of the absorption curves. On account of the requirement of a four-fold site, Zr_4, for the above scheme, this is not unexpected.

According to the PES calculations, the following reaction scheme

$$\mathrm{CH_4}(g) + 2\,\mathrm{S} \xrightarrow{k_1} \underset{n_{CH_3}}{\text{S-CH}_3(a)} + \underset{n_H}{\text{S-H}(a)} \tag{16}$$

$$\text{S-CH}_3(a) + 2\,\mathrm{S} \xrightarrow{k_2} \underset{n_{CH}}{\text{S-CH}(a)} + 2\,\text{S-H}(a) \tag{17}$$

$$\text{S-CH}(a) + \mathrm{S} \xrightarrow{k_3} \underset{n_C}{\text{S-C}(a)} + \text{S-H}(a) \tag{18}$$

is also considered plausible. Consequently the methane absorption process is now described by

$$-(\frac{n_{\mathrm{CH_4}}}{d\,t}) = k_1 n_{CH_4}(s_0 - n_{CH_3} - n_{CH} - n_C)^2 \tag{19}$$

$$(\frac{n_{CH_3}}{d\,t}) = (k_1 n_{CH_4} - k_2 n_{CH_3})(s_0 - n_{CH_3} - n_{CH} - n_C)^2 \tag{20}$$

$$(\frac{n_{CH}}{d\,t}) = k_2 n_{CH_3}(s_0 - n_{CH_3} - n_{CH} - n_C)^2 - k_3 n_{CH}(s_0 - n_{CH_3} - n_{CH} - n_C) \tag{21}$$

$$(\frac{n_C}{d\,t}) = k_3 n_{CH}(s_0 - n_{CH_3} - n_{CH} - n_C) \tag{22}$$

These equations, however, could not give any meaningfull solution because of too many unknown parameters.

To reduce the number of unknown parameters, it was assumed that CH(a) reacts with each other to form carbonaceous deposits on the surface. In addition, the surface concentration of CH(a) was assumed to be negligibly small in comparison to that of the others. Under these

assumptions, the reaction scheme can be simplified to

$$CH_4(g) + 2\,S \xrightarrow{k_1} \underset{n(CH_3)}{S\text{-}CH_3(a)} + \underset{n(H)}{S\text{-}H(a)} \tag{23}$$

$$S\text{-}CH_3(a) + 2\,S \xrightarrow{k_2} \underset{n(CH)}{S\text{-}CH(a)} + 2\,S\text{-}H(a) \tag{24}$$

$$2\,S\text{-}CH(a) \overset{k_3}{\rightsquigarrow} \underset{n(cd)}{S\text{-}CH_n(a)} \tag{25}$$

and solved by the following equations

$$-(\frac{n_{CH_4}}{d\,t}) = k_1 n_{CH_4}(s_0 - n_{CH_3} - n_{cd})^2 \tag{26}$$

$$(\frac{n_{CH_3}}{d\,t}) = (k_1 n_{CH_4} - k_2 n_{CH_3})(s_0 - n_{CH_3} - n_{cd})^2 \tag{27}$$

$$(\frac{n_{cd}}{d\,t}) = k_2 n_{CH_3}(s_0 - n_{CH_3} - n_{cd})^2 - k_3 n_{CH}^2 \tag{28}$$

It was found, however, that the above equations could not be fitted to any of the experimentally observed methane absorption curves. The above equations gave simulation curves which showed monotonical reduction of the absorption rate with time; the absorption curves asymptotically approaching a given level at an early stage of absorption. They thus did not reproduce the latter half of the curves, where the absorption was accelerated. This acceleration of absorption was typically observed in the last half stage of the absorption at high temperatures.

3.4.2. Modified kinetic model

With respect to the appearance of the accelerated absorption, it should be mentioned here that growth of carbonaceous deposits of three-dimensional forms has been observed for catalytic reactions of hydrocarbons on metal surfaces[11]. On account of such observations, growth of carbonaceous deposits was considered to take place similarly for the methane absorption process on Zr-Ni alloys. Accordingly it was assumed that the carbonaceous deposits are formed from CH(a) and C(a) and they take part in the reduction of surface coverage by growing in three dimensions. Providing n_{cd} be the number of molecule of the carbonaceous deposits growing semispherically, its surface coverage should be proportional to $n_{cd}^{3/2}$ because the number of adsorbed and/or deposited molecules are assumed to be proportional to the area covered by them in the above reaction schemes. The modified equations under these assumptions is described as

$$-(\frac{n_{CH_4}}{d\,t}) = k_1 n_{CH_4}(s_0 - n_{CH_3} - n_{cd}^{3/2})^2 \tag{29}$$

$$(\frac{n_{CH_3}}{d\,t}) = (k_1 n_{CH_4} - k_2 n_{CH_3})(s_0 - n_{CH_3} - n_{cd}^{3/2})^2 \tag{30}$$

$$(\frac{n_{CH}}{d\,t}) = [k_2 n_{CH_3}(s_0 - n_{CH_3} - n_{cd}^{3/2}) - k_3 n_{CH}](s_0 - n_{CH_3} - n_{cd}^{3/2}) \tag{31}$$

for the reaction scheme described by reactions (23), (24) and (25).

Figure 5 compares calculated absorption curves for Zr with the observed ones, where the closed circles represent observed data and solid lines show absorption curves simulated from the evaluated rate constants, k_1, k_2 and k_3. The rate constant, k_1 could be determined from the slope of the initial part of observed absorption curves and the other rate constants, i.e. k_2 and k_3, were evaluated by trial-and-error fitting. It is seen in this figure that the calculated absorption curves agree very well with the observed ones, indicating that the above reaction scheme is adequate for describing the kinetics of methane absorption for Zr. It should be mentioned here that the simulation could also reproduce well the convex part of the absorption curves appearing in the latter half of the absorption curves at high temperatures. According to the above-mentioned scheme, the acceleration of the absorption is attributed to the $n_{cd}^{3/2}$ term, which is assigned to the growth of the carbonaceous deposits on the surface in three dimensions.

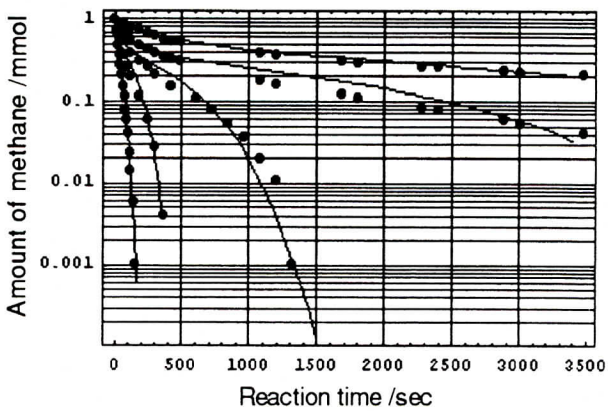

Fig. 5. Comparison of simulated absorption curves with observed ones for Zr at 350, 400, 450, 500 and 550 C (from upper to lower)

With respect to the methane absorption by Zr_4Ni and Zr_2Ni, the active centers for the absorption should not be Zr alone but they are considered to consist of Zr and Ni atoms. Nevertheless it was assumed that the same reaction scheme as the above is valid in these cases.

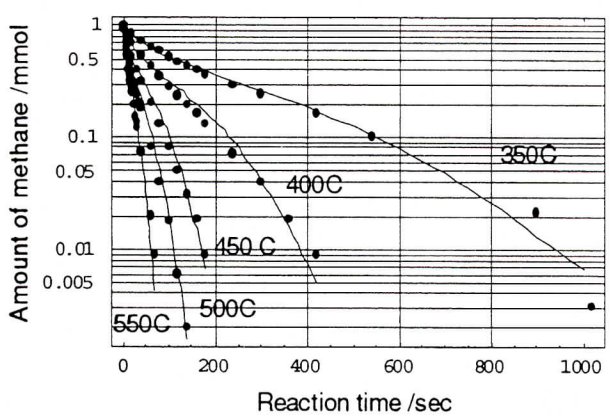

Fig. 6. Comparison of simulated absorption curves with observed ones for Zr_2Ni

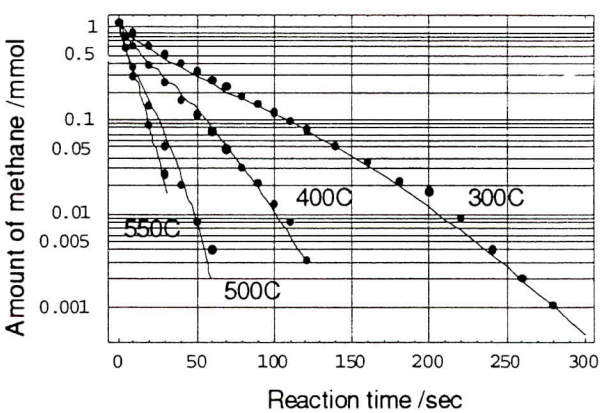

Fig. 7. Comparison of simulated absorption curves with observed ones for Zr_4Ni

Figures 6 and **7** show the results of simulations for the absorption by Zr_4Ni and Zr_2Ni, respectively, where the procedures to obtain simulation curves were the same as those adopted for Zr. It was found that the kinetic equations from (29) to (31) could also reproduce quite well the observed methane absorption curves for Zr_4Ni and Zr_2Ni at different temperatures,

3.4.3. Temperature dependence of the rate constants

Figure 8 shows the temperature dependence of the rate constants, k_1, k_2 and k_3, evaluated from the data analysis for the methane absorption by Zr. All of them exhibited fairly well linear straight lines against 1/T, from which the respective activation energies were calculated as 70.9, 58.5 and 125.5 kJ/mol for k_1, k_2 and k_3, respectively. Although these values are far smaller than those estimated from PES calculations by Gaussian-03, a trend indicating that the activation energy of k_1 is larger than that of k_2 is apparent. The large discrepancy between the activation energies determined from experimental results and from PES calculations can be ascribed to over-simplification of cluster models for PES calculations.

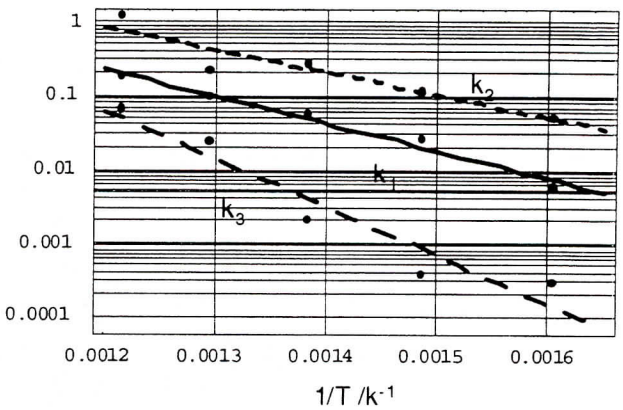

Fig. 8. Arrhenius plot of the rate constants, k_1, k_2 and k_3, evaluated for Zr: the dimensions are $1/mmol^2.sec$ for k_1 and k_2, and $1/mmol.sec$ for k_3

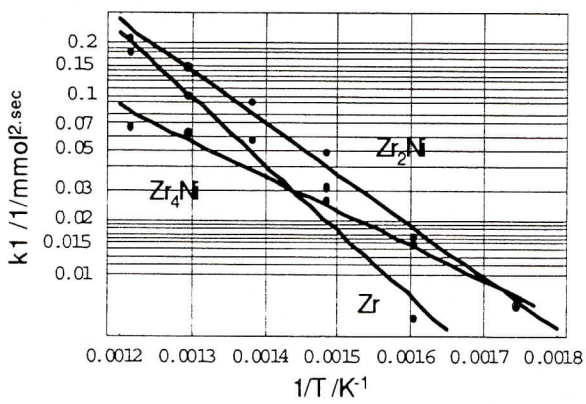

Fig. 9. Arrhenius plot of k_1 evaluated for Zr, Zr_4Ni and Zr_2Ni

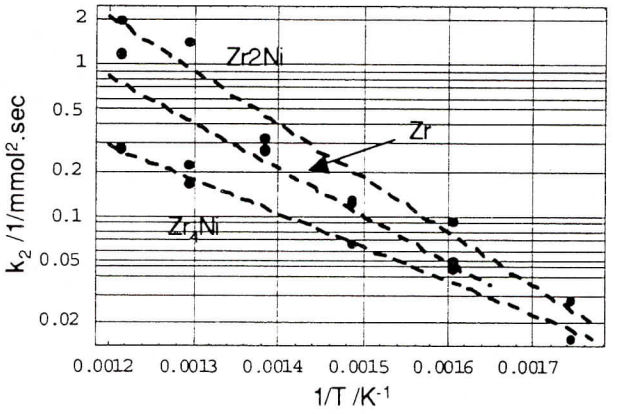

Fig. 10. Arrhenius plot of k_2 evaluated for Zr, Zr_4Ni and Zr_2Ni

Figures 9, 10 and **11** show the temperature dependence of the rate constants, k_1, k_2 and k_3, respectively, that were evaluated for Zr, Zr_2Ni and Zr_4Ni. It is seen in Fig. 9, that although Zr_2Ni has the largest k_1, the values of k_1 are not so much different for the various materials (see Figs.5, 6 and 7). This is contradictory to the results reported in a previous paper[1], in which a large difference of absorption rate constants was reported for Zr, Zr_4Ni, and Zr_2Ni.

The large difference is also apparent from Figs.5, 7 and 6, which show the time required for 90% reduction of the charged methane to be approximately 2500, 110 and 550 seconds at 400°C for Zr, Zr_4Ni and Zr_2Ni, respectively. In addition, according to the present data analysis, the activation energy for dissociative adsorption of CH_4 differs among the three materials; it was determined to be 70.9, 37.2, and 55.3 kJ/mol for Zr, Zr_4Ni, and Zr_2Ni, respectively. These

results are contradictory to the previous paper[1], where the activation energy for methane absorption was evaluated to be around 49 kJ/mol for all of these materials. This is because the apparent absorption rate constants, k, were determined from the slopes of the first part of $\ln P$ vs t plots in the previous paper, and accordingly detailed difference among different materials in their Arrhenius plots are considered to be averaged out, giving similar values for different materials.

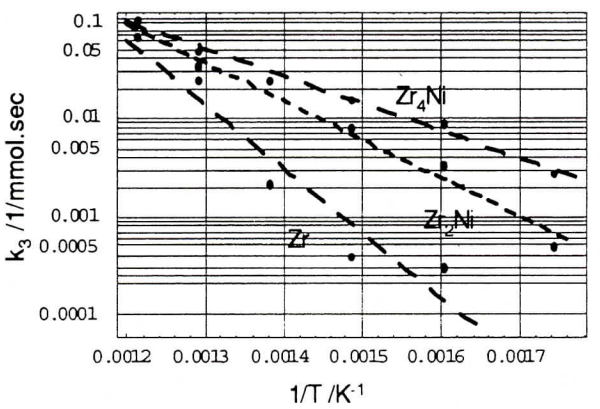

Fig. 11. Arrhenius plot of k_3 evaluated for Zr, Zr_4Ni and Zr_2Ni

The activation energy for k_2 was evaluated to be 58.5, 42.3, and 67.7 kJ/mol and that for k_3 was 125.5, 53.4, and 74.8 kJ/mol. for Zr, Zr_4Ni, and Zr_2Ni, respectively. It should be mentioned that the largest value of k_2 was observed for Zr_2Ni, and Zr_4Ni gave the smallest one. This is not consistent with the activity order of $Zr_4Ni > Zr_2Ni > Zr$. On the other hand, Zr_4Ni gave the largest k_3 value and Zr the smallest value; this feature is the same as the activity order of $Zr_4Ni > Zr_2Ni > Zr$. These observations indicate that the overall activity for the decomposition/absorption of methane is determined by k_3: k_1 and k_2 play minor roles for absorption of methane, especially methane removal of more than 90%. It can be concluded that the aggregation of carbonaceous residues responsible for the three-dimensional growth of carbonaceous deposits on the surface governs the activity for methane absorption as a whole.

4. Conclusions

The kinetics of methane absorption by Zr, Zr_2Ni, and Zr_4Ni was analyzed over the entire range of the absorption curves by taking account of plausible elementary reactions, which were inspected by potential energy surfaces(PESs) of relevant reactions calculated with the Gaussian 03 package. The kinetic analysis and PES calculation revealed that the absorption/decomposition of methane proceeds via the reactions $CH_4(g) \xrightarrow{k_1} CH_3(a) \xrightarrow{k_2} CH(a) \xrightarrow{k_3}$ C-deposits. The absorption curves down to 99.9% consumption of the initially loaded amount of methane could be reproduced using the rate constants, k_1, k_2 and k_3, which were evaluated from curve-fitting of the observed absorption curves by considering a series of differential equations describing the elementary reactions.

It was found that the values of the three rate constants are dependent on the materials, but only the order of magnitude of k_3 is consistent with the experimentally observed order of activity for the absorption beyond 90% consumption of the initially loaded methane. This indicates that the first and second step of the reaction series described above play only minor

roles; the overall absorption reactivity (methane consumption beyond 90%) of the materials is governed by the final third step.

References

[1] K. Watanabe, W. M. Shu, M. Motohashi, and M. Matsuyama, *Fusion Engn. Design*, 39/40 (1998) 1055 –1060

[2] L. C. Emerson, R. J. Knize, J. L. Cecchi, and O. Auciello, *J. Vac. Sci. Technol.*, A4 (1986) 297–299

[3] L. C. Emerson, R. J. Knize, and J. L. Cecchi, *J. Vac. Sci. Technol.*, A5 (1987) 2584–2586

[4] W. M. Shu, M. Matsuyama, and K. Watanabe, *Ann. Rept. HRC., Toyama Univ.*, 16 (1996) 59–68

[5] M. Matsuyama, E. Motohashi, W. M. Shu, and K. Watanabe, *Ann. Rept. HRC., Toyama Univ.*, 17 (1997) 73–84

[6] M. J. Frisch, G. W. Trucks, H. B. Schlegel, G. E. Scuseria, M. A. Robband J. R. Cheesemanand J. A. Montgomeryand Jr.and T. Vrevenand K. N. Kudinand J. C. Burantand J. M. Millamand S. S. Iyengarand J. Tomasiand V. Baroneand B. Mennucciand M. Cossiand G. Scalmaniand N. Regaand G. A. Peterssonand H. Nakatsujiand M. Hadaand M. Eharaand K. Toyotaand R. Fukudaand J. Hasegawaand M. Ishidaand T. Nakajimaand Y. Hondaand O. Kitaoand H. Nakaiand M. Kleneand X. Liand J. E. Knoxand H. P. Hratchianand J. B. Crossand C. Adamoand J. Jaramilloand R. Gompertsand R. E. Stratmannand O. Yazyevand A. J. Austinand R. Cammiand C. Pomelliand J. W. Ochterskiand P. Y. Ayalaand K. Morokumaand G. A. Vothand P. Salvadorand J. J. Dannenbergand V. G. Zakrzewskiand S. Dapprichand A. D. Danielsand M. C. Strainand O. Farkasand D. K. Malickand A. D. Rabuckand K. Raghavachariand J. B. Foresmanand J. V. Ortizand Q. Cuiand A. G. Babouland S. Cliffordand J. Cioslowskiand B. B. Stefanovand G. Liuand A. Liashenkoand P. Piskorzand I. Komaromiand R. L. Martinand D. J. Foxand T. Keithand M. A. Al-Lahamand C. Y. Pengand A. Nanayakkaraand M. Challacombeand P. M. W. Gilland B. Johnsonand W. Chenand M. W. Wongand C. Gonzalezand, and J. A. Popleand, *Gaussian03, RevisionB.03.* Gaussian Inc.and Pittsburgh, 2003.

[7] L. Wan, R. Hayakawa, Y. Hatano, and K. Watanabe, *Ann. Rept. HRC. Toyama Univ., Japan*, 23 (2003) 29–41

[8] Y. Jin, L. Wan, M. Hara, Y. Hatano, and K. Watanabe, *Mater. Trans.*, 48 (2007) 560–565

[9] The Japan Institute of Metals, *Metal Databook*, 2nd Ed. (in Japanese), Muruzen, Tokyo, Japan, 1984

[10] Y. Fukai, K. Tanaka and H. Uchida, *Hydrogen and Metals* (in Japanese), Uchida Roukakuho, Japan, 1998

[11] R. T. K. Baker and R. J. Waite, *J. Catal.*, 37 (1975) 101–105